Chinese Chemical Letters 34 (2023) 108086

Contents lists available at ScienceDirect

Chinese Chemical Letters

journal homepage: www.elsevier.com/locate/cclet

Lanthanide coordinated multicolor fluorescent polymeric hydrogels for bio-inspired shape/color switchable actuation through local diffusion of Tb^{3+}/Eu^{3+} ions

Ruijia Wang[a,b], Wei Lu[b,*], Yi Zhang[b], Wanning Li[b], Wenqin Wang[a,*], Tao Chen[b,*]

[a] Faculty of Materials Science and Chemical Engineering, Ningbo University, Ningbo 315211, China
[b] Key Laboratory of Marine Materials and Related Technologies, Zhejiang Key Laboratory of Marine Materials and Protective Technologies, Ningbo Institute of Material Technology and Engineering, Chinese Academy of Sciences, Ningbo 315201, China

ARTICLE INFO

Article history:
Received 8 October 2022
Revised 5 December 2022
Accepted 16 December 2022
Available online 17 December 2022

Keywords:
Multicolor fluorescence
Polymeric hydrogel
Lanthanide coordination
Actuator
Fluorescent patterns

ABSTRACT

Lanthanide coordinated multicolor fluorescent polymeric hydrogels (MFPHs) are quite promising for various applications because of their sharp fluorescence bands and high color purity. However, few attempts have been carried out to locally regulate their fluorescence switching or shape deforming behaviors, but such studies are very useful for patterned materials with disparate functions. Herein, the picolinate moieties that can sensitize Tb^{3+}/Eu^{3+} luminescence *via* antenna effect were chemically introduced into interpenetrating double networks to produce a robust kind of lanthanide coordinated MFPHs. Upon varying the doping ratio of Tb^{3+}/Eu^{3+}, fluorescence colors of the obtained hydrogels were continuously regulated from green to orange and then red. Importantly, spatial fluorescence color control within the hydrogel matrix could be facilely realized by controlled diffusion of Tb^{3+}/Eu^{3+} ions, producing a number of 2D hydrogel objects with local multicolor fluorescent patterns. Furthermore, the differential swelling capacities between the fluorescent patterned and non-fluorescent parts led to interesting 2D-to-3D shape deformation to give well-defined multicolor fluorescent 3D hydrogel configurations. Based on these results, bio-inspired synergistic color/shape changeable actuators were demonstrated. The present study provided a promising strategy to achieve the local fluorescence and shape control within lanthanide coordinated hydrogels, and is expected to be expanded for fabricating useful patterned materials with disparate functions.

Multicolor fluorescent polymeric hydrogels (MFPHs) are found to have many promising applications such as bioimaging [1–3], sensing [4–8] and soft actuators/robotics [9–13], as they are capable of featuring responsive changes in both emission intensity and color. Usually, MFPHs are produced by the chemical bonding or physical doping of two or more responsive fluorogens into a single hydrophilic hydrogen matrix [14–21]. The past five years have witnessed a number of MFPHs based on organic fluorophores [22–25], fluorescent proteins [26,27], lanthanide complexes [28–30] or luminescent nanoparticles [31–35]. Among them, lanthanide-coordinated MFPHs are particularly attracting our interests because lanthanide luminescence has many unique merits, *e.g.*, sharp fluorescence bands, high color purity and good photochemical stability [36–38]. In this context, several MFPHs have been recently presented by supramolecular assembly of polycations with lanthanide coordination polyanions or copolymerization of lanthanide complexes into cross-linked polymer network [39–43]. These impressive advances have largely enriched the family of lanthanide coordinated MFPHs and promoted their development for various demonstrated uses.

In these current studies, fluorescent intensities and colors of the whole hydrogels were globally varied [36,44,45]. Few efforts have been conducted to locally tune their fluorescent behaviors for spatial emission control on/within hydrogels, but such attempt is very useful. For one thing, the capacity for spatial fluorescence control is able to creating patterned heterogenetic and periodic structures on 2D hydrogel sheet for providing well-defined areas with disparate functions [46]. For another, such patterned structures stabilized by lanthanide coordination crosslinks potentially cause their differential swelling ratios with other areas [47,48]. As a result, responsive 2D-to-3D shape deforming functions may be further achieved accompanying with simultaneous fluorescence intensity

* Corresponding authors.
E-mail addresses: luwei@nimte.ac.cn (W. Lu), wangwenqin@nbu.edu.cn (W. Wang), tao.chen@nimte.ac.cn (T. Chen).

https://doi.org/10.1016/j.cclet.2022.108086
1001-8417/

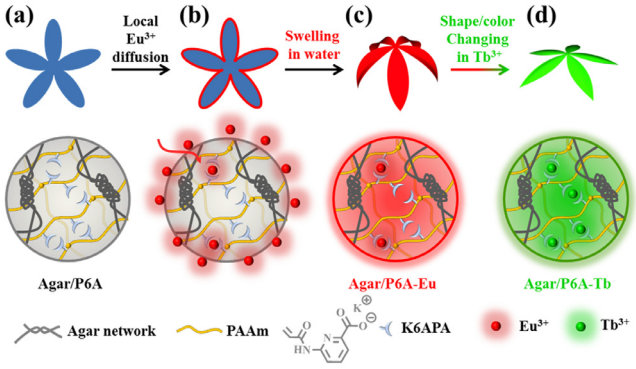

Scheme 1. (a) The flower-shaped Agar/P6A hydrogel object and its chemical structure. (b) Local diffusion of Eu^{3+} into the hydrogel matrix from the hydrogel edge. (c) 2D-to-3D shape deformation of the flower-shaped hydrogel due to the differential swelling capacities between the outer and inner parts. (d) Synergistic shape and color changing actuation in aqueous Tb^{3+} solution.

and color responses. These advantages would potentially enrich the functions of lanthanide coordinated MFPHs. However, such attempt to fabricate lanthanide coordinated MFPHs with spatial emission control has been largely ignored.

Herein, we took advantage of dynamic Tb^{3+}/Eu^{3+} coordination interactions to present robust MFPH systems, and realized efficient spatial control of their emission intensity and color, followed by exploring their potential for bio-inspired synergistic color/shape switchable actuation. As illustrated in Scheme 1a, the prepared hydrogel (Agar/P6A) is composed of the chemically crosslinked poly(potassium 6-acrylamidopicolinate-*co*-acrylamide) (P6A) containing coordinative picolinate moieties and the hydrogen bonded Agar network. Taking advantage of Eu^{3+}-picolinate coordination, aqueous Eu^{3+} solution was allowed to locally diffuse into the outer part of the Agar/P6A hydrogel object to achieve spatial emission color control in the hydrogel matrix (Scheme 1b). Subsequently, 2D-to-3D shape deformation was achieved in water because of the differential swelling capacities between the outer and inner parts with different crosslinking density (Scheme 1c). Consequently, bio-inspired synergistic shape deforming and color changing behaviors were realized when treating the obtained 3D hydrogel configuration in aqueous Tb^{3+} solution (Scheme 1d). This is because the abundant Tb^{3+} ions spontaneously diffused into the hydrogel matrix to not only transform the red fluorescent Eu^{3+}-picolinate complex to green fluorescent Tb^{3+}-picolinate complex, but also eliminate the swelling capacities between different parts of the hydrogel.

Fig. 1a depicts the general procedure to produce the multicolor fluorescent polymeric hydrogels. Briefly, all reactants, including agar polymer, acrylamide (AAm), potassium acrylamidopicolinate (K6APA), methylene diacrylamide crosslinker and potassium persulfate (KPS, the initiator), were completely dissolved in hot deionized water, and then cooled down to room temperature for 30 min. During the cooling time, physically crosslinked agar network was formed *via* hydrogen bond-associated agar helix bundles. Then, the thermal radical polymerization was initiated to produce the chemically crosslinked P6A network that interpenetrates with the first agar network. The as-prepared double-network Agar/P6A is transparent and colorless under day light (Fig. S1 in Supporting information). Its film (thickness ~2 mm) only exhibits a strong UV absorbance band of the incorporated picolinate moiety around 330 nm (Fig. S2 in Supporting information), and thus has a transmittance above 75% over the whole visible light range. Under 254-nm UV light, weak blue fluorescence was observed (Fig. S3 in Supporting information), as is evidenced by the appearance of the

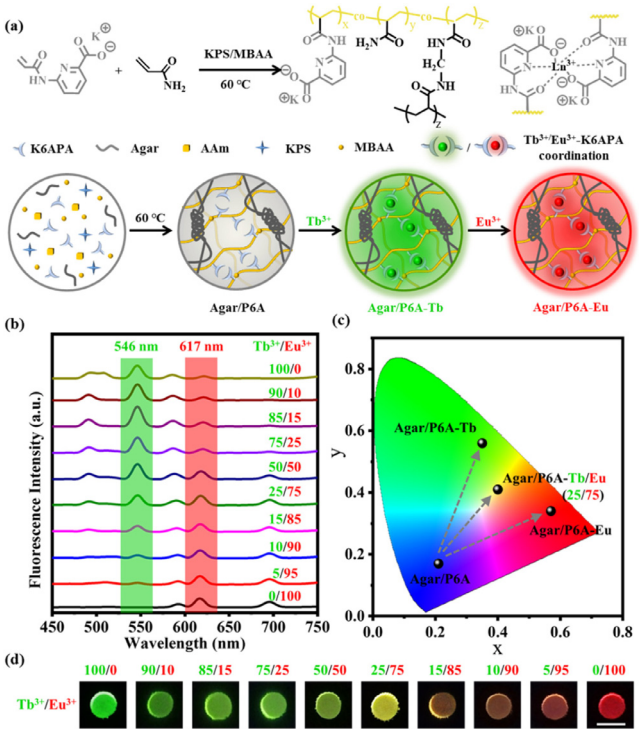

Fig. 1. Preparation of the multicolor fluorescent polymeric hydrogels (Agar/P6A-Tb/Eu). (a) Illustration showing the synthetic procedure of Agar/P6A and Agar/P6A-Tb/Eu hydrogels. (b) Fluorescence spectra of the Agar/P6A-Tb/Eu hydrogels with varied Tb^{3+}/Eu^{3+} molar ratio. Excitation at 254 nm for the fluorescence spectral measurements. (c) CIE (1931) coordinate diagrams of Agar/P6A and Agar/P6A-Tb/Eu hydrogels. (d) Photos of the Agar/P6A-Tb/Eu hydrogels with varied Tb^{3+}/Eu^{3+} molar ratio, which were taken under a 254 nm UV lamp. Scale bars: 5 mm.

broad emission band ranging from 350 nm to 450 nm in the fluorescence spectrum of Agar/P6A hydrogel.

To produce multicolor fluorescence, Agar/P6A hydrogel was globally treated in the aqueous solutions of Eu^{3+}, Tb^{3+} or their mixture to introduce the red or green fluorescent centers (K6APA-Eu or K6APA-Tb). SEM images of Agar/P6A and Agar/P6A-Eu/Tb hydrogels indicated different porous structures, suggesting the formation of lanthanide coordination crosslinks (Fig. S4 in Supporting information). As shown in Fig. S3 and Fig. 1b, strong green and red fluorescent bands were observed around 546 nm and 617 nm in the fluorescence spectra of Agar/P6A-Tb and Agar/P6A-Eu hydrogels, respectively. It was also found that these new green and red emission bands appeared at the cost of the significant decline of the blue fluorescence band, suggesting the energy transfer process from the picolinate ligand to the center lanthanide ions. This observation clearly demonstrated that the intense green and red fluorescence originated from the introduced K6APA-Tb or K6APA-Eu complexes. As expected, it is very facile to modulate the fluorescence color of the Agar/P6A-Eu/Tb hydrogels by simply varying the Tb^{3+}/Eu^{3+} molar ratio (Fig. S5 in Supporting information). As demonstrated in Figs. 1c and d, the fluorescence color of Agar/P6A-Eu/Tb gradually changes from green to yellow, orange and red upon decreasing the Tb^{3+}/Eu^{3+} molar ratio. These diverse-colored fluorescent hydrogels are quite beneficial for the following color-changing hydrogel actuating studies.

Having globally tuned the fluorescence color of the whole hydrogels, we next tried to realize spatial emission color control in the hydrogel matrix. To this end, aqueous Tb^{3+}/Eu^{3+} solution was allowed to gradually diffuse into the hydrogel object. As shown in Fig. 2a, when aqueous Eu^{3+} and Tb^{3+} solution (0.1 mol/L) was respectively added in the outer and inner space of one circular ring-

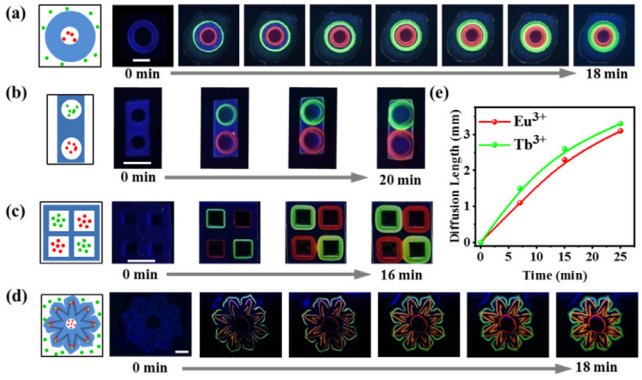

Fig. 2. Spatial fluorescence color control within the Agar/P6A hydrogel matrix through local Eu^{3+}/Tb^{3+} diffusion. (a-d) Photos showing the time-dependent fluorescent color change within the hydrogel matrix. (e) The diffusion kinetics of Eu^{3+} and Tb^{3+} in the hydrogel at room temperature. All pictures were taken under a 254 nm UV lamp. Scale bars: 10 mm.

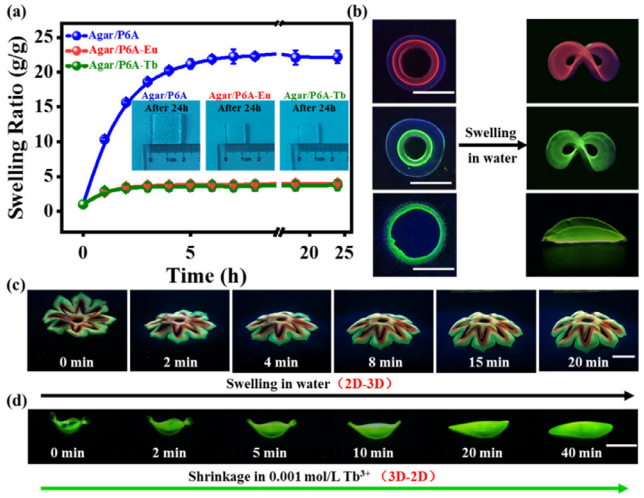

Fig. 3. Shape deformation of the patterned hydrogel objects. (a) The swelling kinetics of Agar-P6A and Agar/P6A-Eu/Tb in water at room temperature. (b) Photos showing the 2D-to-3D shape deformation of the patterned hydrogel objects in water. (c) Photos showing the 2D-to-3D shape deformation of the flower-shaped hydrogel object swelling in water. (d) Photos showing the saddle-like 3D hydrogel shrinking into a 2D sheet hydrogel in the aqueous solutions of Tb^{3+}. All pictures were taken under a 254 nm UV lamp. Scale bars: 10 mm.

shaped Agar/P6A hydrogel, Eu^{3+} and Tb^{3+} would spontaneously diffuse into the hydrogel due to concentration difference. Owing to the lanthanide luminescence sensitization of K6APA moieties, such time-dependent diffusion process could be directly observed under 254-nm UV light, resulting in the formation of distinct hydrogel objects if the diffusion process was stopped at different time. Following a similar line, round-shaped or other shaped hydrogel blocks with two or more round/square cutouts were also utilized to prepare luminescent hydrogel objects with spatial fluorescence control (Figs. 2b-d, Fig. S6, Movies S1 and S2 in Supporting information). Further researches also indicated quite good stability of these fluorescent patterns (Fig. S7 in Supporting information). Quantitative study of these processes revealed that Eu^{3+} and Tb^{3+} solutions (0.1 mol/L) have similar diffusion kinetics at room temperature with an average speed of 7.2 mm/h due to the similar ionic sizes and charge quantity of these two lanthanide ions (Fig. 2e). Moreover, the diffusion speed of Tb^{3+}/Eu^{3+} ions in the hydrogels could be regulated by facilely varying their concentration or the environment temperature (Fig. S8 in Supporting information). Therefore, the line width of these fluorescent patterns could be regulated from hundreds of μm to several cm by delicately controlling the experiment conditions.

Besides spatial fluorescence color control, 2D-to-3D shape deformation of these patterned hydrogel objects was further achieved *via* subsequent swelling in water. As can be seen from the swelling kinetics in Fig. 3a and Fig. S9 (Supporting information), the differential swelling capacities between Agar-P6A and Agar/P6A-Eu/Tb lays the foundation for the subsequent 2D-to-3D shape deformation. As for the patterned hydrogel samples shown in Fig. 3b and Fig. S10 (Supporting information), the blue fluorescent part was highly swollen, while the green or red fluorescent part was less swollen because of the additional Tb^{3+}/Eu^{3+} coordinated crosslinks. According to the equilibrium deduced from Flory-Huggins lattice model theory in Note 1 (Supporting information), the crosslinking degree is positively related to the swelling degree. Therefore, the different crosslinking density between outer and inner hydrogel parts led to differential swelling capacities in water, which thus induced out-of-plane deformation of the initial 2D hydrogel into 3D hydrogel structure. This strategy could also be applied to hydrogel sheets with more complex fluorescent patterns. Fig. 3c and Fig. S11 (Supporting information) depict a flower-shaped 2D hydrogel sheet with different colors, in which the internal stamen part and external petal part were doped by Eu^{3+} and Tb^{3+} ions, respectively. After being immersed in water, the differential swelling extent between the inner red and outer green fluorescent parts and middle blue fluorescent parts forced the initial 2D hydrogel to gradually deform into a complex 3D hydrogel configuration (Movie S3 in Supporting information). Also, the shape deformation of 3D hydrogel configuration could be restored to the isotropic 2D sheet shape. For example, when the saddle-shaped 3D configuration was put into aqueous Tb^{3+} solution, the 3D profile was gradually restored to 2D hydrogel sheet because the whole fluorescent hydrogel was fully coordinated by excessive Tb^{3+} ions to reach the isotropic state (Fig. 3d and Movie S4 in Supporting information). These demonstrated examples suggest the great potential of the proposed strategy to prepare complex 3D hydrogel structures through pre-designed spatial emission color control.

Enlightened by the above-established multicolor fluorescence and controlled 2D-to-3D and 3D-to-2D shape deformation, we finally explored the possibility to fabricate bio-inspired synergistic shape/color switchable hydrogel actuators, because such multifunctional actuation poses many potential uses for soft display, camouflaged soft robotics, *etc.* As a proof-of-concept, a flower-shaped hydrogel was cut by a laser cutting machine and Eu^{3+} would locally diffuse into the hydrogel from the outside due to concentration difference (Fig. S12 in Supporting information). After diffusion for 5 min, the Agar/P6A-Eu was put into water and swelled into an arched configuration after 12 min (Fig. 4a and Movie S5 in Supporting information). When placed in 0.001 mol/L aqueous Tb^{3+} solution, the red 3D arched configuration gradually converted into a green 2D flat shape due to the Tb^{3+} diffusion into the highly swollen region and replaced Eu^{3+}. Similarly, leaf-shaped hydrogel switching from 3D green crimped configuration into 2D red flat sheet shape was also demonstrated (Fig. 4b, Fig. S13 and Movie S6 in Supporting information).

In conclusion, we have presented a robust kind of multicolor fluorescent polymeric hydrogels based on K6APA-Eu^{3+} or K6APA-Tb^{3+} complexes, and put forth a promising strategy to locally regulate their fluorescence switching or shape deforming behaviors through local diffusion of Tb^{3+}/Eu^{3+} ions. The materials were prepared by copolymerizing a picolinate-functionalized K6APA monomer into the chemically crosslinked poly(K6APA-AAm) network that are interpenetrated with hydrogen bonded agar network. Since K6APA was able to sensitize the red and green luminescence of Eu^{3+} and Tb^{3+} ions *via* antenna effect, various

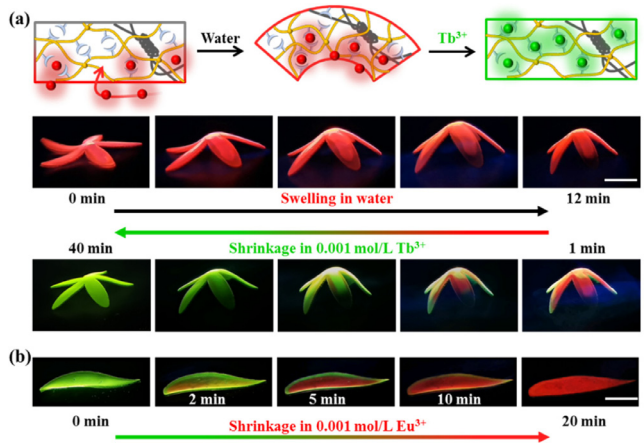

Fig. 4. Bio-inspired synergistic shape/color switchable actuation. (a) Illustration and photos showing 2D-to-3D swelling deformation in water, and simultaneous color/shape changes of the artificial flower-shaped hydrogel actuator in aqueous Tb^{3+} solution. (b) Photos showing synergistic shape deformation and color change of the artificial leaf-shaped hydrogel actuator in aqueous Eu^{3+} solution. All pictures were taken under a 254 nm UV lamp. Scale bars: 10 mm.

multicolor fluorescent patterned 2D hydrogel objects were facilely achieved by the controlled diffusion of Tb^{3+}/Eu^{3+} into the hydrogel. Interestingly, the introduction of additional lanthanide coordinated crosslinks resulted in much less swelling ratio of the fluorescent parts than that of the non-fluorescent parts. Consequently, such patterned 2D hydrogel objects were spontaneously swollen into well-defined 3D hydrogel configurations that are difficult to be obtained by other methods. Based on these results, we further demonstrated the possibility to realize bio-inspired synergistic shape/color switchable actuation that holds wide potential uses in camouflaged soft robotics, information encryption and so on.

Declaration of competing interest

The authors declare that they have no known competing financial interests or personal relationships that could have appeared to influence the work reported in this paper.

Acknowledgments

This research was supported by National Natural Science Foundation of China (No. 52073297), the Sino-German mobility program (No. M-0424), Youth Innovation Promotion Association of Chinese Academy of Sciences (No. 2019297) and K.C. Wong Education Foundation (No. GJTD-2019–13).

Supplementary materials

Supplementary material associated with this article can be found, in the online version, at doi:10.1016/j.cclet.2022.108086.

References

[1] Y. Zhang, C. Li, H. Yang, et al., Sci. China. Tech. Sci. 65 (2021) 191–200.
[2] W. Liu, W. Zhang, X. Yu, G. Zhang, Z. Su, Polym. Chem. 7 (2016) 5749–5762.
[3] J. Li, Z. Wang, H. Han, et al., Chin. Chem. Lett. 33 (2022) 1936–1940.
[4] L. Hu, Q. Zhang, X. Li, M.J. Serpe, Mater. Horiz. 6 (2019) 1774–1793.
[5] F. Diehl, S. Hageneder, S. Fossati, et al., Chem. Soc. Rev. 51 (2022) 3926–3963.
[6] N. Chen, Y. Zhou, Y. Liu, et al., Nano Res. 15 (2022) 7703–7712.
[7] S. Li, J. Ma, X. Zhao, et al., Chin. Chem. Lett. 33 (2022) 1850–1854.
[8] N. Wang, H. Yao, Q. Tao, et al., Chin. Chem. Lett. 33 (2022) 252–256.
[9] B.Y. Wu, X.X. Le, Y.K. Jian, et al., Macromol. Rapid Commun. 40 (2019) 1800648.
[10] M.T.I. Mredha, I. Jeon, Prog. Mater. Sci. 124 (2022) 100870.
[11] C. Ma, W. Lu, X. Yang, et al., Adv. Funct. Mater. 28 (2018) 1704568.
[12] D. Jiao, Q.L. Zhu, C.Y. Li, Q. Zheng, Z.L. Wu, Acc. Chem. Res. 55 (2022) 1533–1545.
[13] J. Fang, Y. Zhuang, K. Liu, et al., Adv. Sci. 9 (2022) 2104347.
[14] S. Wei, Z. Li, W. Lu, et al., Angew. Chem. Int. Ed. 60 (2021) 8608–8624.
[15] Y. Tu, Z. Zhao, J.W.Y. Lam, B.Z. Tang, Matter 4 (2021) 338–349.
[16] H. Qiu, S. Wei, H. Liu, et al., Adv. Intell.Syst. 3 (2021) 2000239.
[17] W. Lu, S. Wei, H. Shi, et al., Aggregate 2 (2021) 37.
[18] W. Lu, M. Si, X. Le, T. Chen, Acc. Chem. Res. 55 (2022) 2291–2303.
[19] Z. Li, X. Ji, H. Xie, B.Z. Tang, Adv. Mater. 33 (2021) 2100021.
[20] H. Xie, Z. Li, J. Gong, et al., Adv. Mater. 33 (2021) 2105113.
[21] X. Le, H. Shang, H. Yan, et al., Angew. Chem. Int. Ed. 60 (2021) 3640–3646.
[22] Z. Wang, J. Nie, W. Qin, Q. Hu, B.Z. Tang, Nat. Commun. 7 (2016) 12033.
[23] C. Madhu, B. Roy, P. Makam, T. Govindaraju, Chem. Commun. 54 (2018) 2280–2283.
[24] X. Liu, B. Li, W. Wang, et al., Chem. Eng. J. 449 (2022) 137718.
[25] H. Chen, F. Yang, Q. Chen, J. Zheng, Adv. Mater. 29 (2017) 1606900.
[26] P. Xie, Y. Zhou, X. Li, et al., Chin. Chem. Lett. 34 (2023) 107582.
[27] M.D. Weber, L. Niklaus, M. Proschel, et al., Adv. Mater. 27 (2015) 5493–5498.
[28] G. Yin, J. Huang, D. Liu, et al., Chin. Chem. Lett. 34 (2023) 107290.
[29] G. Weng, S. Thanneeru, J. He, Adv. Mater. 30 (2018) 1706526.
[30] S. Cheng, Z. Chen, Y. Yin, Y. Sun, S. Liu, Chin. Chem. Lett. 32 (2021) 3718–3732.
[31] H. Zhi, X. Fei, J. Tian, et al., J. Mater. Chem. B 5 (2017) 5738–5744.
[32] S. Wu, H. Shi, W. Lu, et al., Angew. Chem. Int. Ed. 60 (2021) 21890–21898.
[33] M. Stupca, O.M. Nayfeh, T. Hoang, et al., J. Appl. Phys. 112 (2012) 074313.
[34] J. Hai, X. Zeng, Y. Zhu, B. Wang, Biomaterials 194 (2019) 161–170.
[35] J. Hai, T. Li, J. Su, et al., Angew. Chem. Int. Ed. 57 (2018) 6786–6790.
[36] S. Wei, W. Lu, X. Le, et al., Angew. Chem. Int. Ed. 58 (2019) 16243–16251.
[37] H. Shi, S. Wu, M. Si, et al., Adv. Mater. 34 (2022) 2107452.
[38] W. Lu, M. Si, H. Liu, et al., Cell Rep. Phys. Sci. 2 (2021) 100417.
[39] H. Wang, X. Ji, Y. Li, et al., J. Mater. Chem. B 6 (2018) 2728–2733.
[40] M. Si, H. Shi, H. Liu, et al., Mater. Chem. Front. 5 (2021) 5130–5141.
[41] C. Ma, T. Li, Q. Zhao, et al., Adv. Mater. 26 (2014) 5665–5669.
[42] H. Liu, S. Wei, H. Qiu, et al., Adv. Funct. Mater. 32 (2021) 2108830.
[43] Z. Li, Z. Hou, H. Fan, H. Li, Adv. Funct. Mater. 27 (2017) 1604379.
[44] M. Nie, C. Huang, X. Du, Nanoscale 13 (2021) 2780–2791.
[45] Z. Li, P. Liu, X. Ji, et al., Adv. Mater. 32 (2020) 1906493.
[46] P. Li, D. Zhang, Y. Zhang, et al., ACS Macro Lett. 8 (2019) 937–942.
[47] X.P. Hao, Z. Xu, C.Y. Li, et al., Adv. Mater. 32 (2020) 2000781.
[48] H. Guo, J. Chen, Z. Wang, et al., Chin. Chem. Lett. 33 (2022) 2178–2182.